Journal of Molecular Catalysis A: Chemical 415 (2016) 65–73

Contents lists available at ScienceDirect

Journal of Molecular Catalysis A: Chemical

journal homepage: www.elsevier.com/locate/molcata

Amidase activity of phosphonate analogue imprinted chymotrypsin mimics in shape-selective, substrate-specific and enantioselective amidolysis of L-phenylalanine-*p*-nitroanilides

Divya Mathew [a], Benny Thomas [a,b], K.S. Devaky [a,*]

[a] School of Chemical Sciences, Mahatma Gandhi University, Kottayam 686 560, India
[b] Department of Chemistry, St. Berchmans College, Changanacherry, 686 101, India

ARTICLE INFO

Article history:
Received 31 March 2015
Received in revised form
17 December 2015
Accepted 23 January 2016
Available online 27 January 2016

Keywords:
Molecularly imprinted enzyme mimics
Amidase activity
Transition state analog
Shape-selective amidolysis
Catalytic efficiency
Michaelis–Menten kinetics
Enantioselectivity
Imprinting efficiency
Memorized cavity

ABSTRACT

Focusing on chymotrypsin mimics, highly crosslinked enzyme mimics are synthesized by molecular imprinting technique for the amidolysis of *p*-nitroanilide of phenylalanine, using phenyl-1-(*N*-benzyloxycarbonylamino)-2-(phenyl)ethyl phosphonate – the transition state analog of amidolysis – as the template, *N*-methacryloyl-L-histidine, *N*-methacryloyl-L-aspartic acid, and *N*-methacryloyl-L-serine as the functional monomers and EGDMA as the crosslinking agent. The amidase activity of the enzyme mimics follows pseudo first order kinetics. The transition state analog provides a tetrahedral geometry complementary to the transition state intermediate, which is responsible for the catalytic activity of the imprinted enzyme mimics. The enzyme mimics show stereospecificity and substrate selectivity in the amidolysis of phenylalanine *p*-nitroanilide. The proper orientation of the reactive functionalities in the super crosslinked macroporous polymer matrix for selective binding of the substrate through H-bonding is responsible for the high imprinting efficiency and substrate specificity of the imprinted polymer catalysts. Low cost, ease of preparation, high thermal stability, reusability and higher shelf life make the polymer catalysts better chymotrypsin mimics.

1. Introduction

The fabrication of synthetic enzyme mimics by molecular imprinting technique – the creation of tailor made binding sites with memory of the shape, size and functional groups of the template molecule – has spanned the area of research to conquer the practical borders of biological enzymes like denaturation in organic solvents, instability against high temperatures, severe pH conditions, difficulties in isolation, loss of activity on recycling etc [1–3]. In the molecular imprinting process, the template is of vital significance, which directs the organization of the functional groups pendent to the functional monomers, the complete removal of the template molecule creates specific recognition sites complementary to the size, shape, and chemical functionalities of the template molecule [4–7]. Super-crosslinked nature of the three-dimensional recognition site is responsible for the binding specificity and lot of applications like chromatographic separation, sensors, drug delivery, recognition of peptides etc [8–10].

Most of the studies have focused on the enzyme chymotrypsin, which specifically hydrolyses esters or amides comprising of phenylalanyl or tyrosyl residues as a part of the carbonyl group [11,12]. The environment of the active site and mechanism of its hydrolytic action are well understood, that the nucleophilicity of serine hydroxyl group is enhanced by the co-operative action of the imidazole moiety of histidine and carboxylic group of aspartic acid, which are buried in a hydrophobic pocket [13,14]. Even though there are many reports on imprinted and non-imprinted polymer catalyzed esterolytic reactions, amide or peptide hydrolysis reactions using artificial enzyme mimics are less reported. In the present paper, we report the synthesis of a series of chymotrypsin mimics and studies on their catalytic activity in the amidolysis of *p*-nitroanilides of phenylalanine highlighting the co-operative effect of functional monomers in the imprinted polymer. The substrate specificity and stereo selectivity of the enzyme mimics, effect of the structure of the imprinted TSA on the catalytic activity etc. are illustrated.

* Corresponding author at: School of Chemical Sciences, Mahatma Gandhi University, Priyadarshini Hills P.O., Kottayam 686 560, Kerala, India. Fax: +91 481 2731002.
E-mail address: ksdevakyscs@yahoo.com (K.S. Devaky).

http://dx.doi.org/10.1016/j.molcata.2016.01.029
1381-1169/

2. Experimental

2.1. Materials and methods

Dicyclohexylcarbodiimide (DCC), ethylene glycol dimethacrylate (EGDMA) and phenethyl boronic acid were purchased from Sigma–Aldrich, USA. α-Chymotrypsin, Z/Boc/Nphth/Fmoc-L-phenylalanine, *Z*-L-alanine, L-histidine, L-serine, L-aspartic acid, benzyl carbamate, triphenyl phosphite and phenylacetaldehyde were purchased from SRL, Mumbai. Other chemicals available from local suppliers were purified prior to use by following the standard procedures.

IR spectra were recorded on a Shimadzu FT-IR-8400S spectrophotometer. Kinetic studies were performed using Shimadzu UV 2450 spectrophotometer. JEOL JSM6390 SEM analyzer was used for SEM analysis. ^{1}H NMR spectra were taken using Bruker Advance DPX-300 MHz FT-NMR spectrometer in $CDCl_3$.

2.2. Synthesis of TSA-A (*phenyl-1-(*N-*benzyloxycarbonylamino)-2-(phenyl)ethyl phosphonate)*

The transition state analog was synthesized by refluxing 4.10 mL, 13.20 mmol triphenyl phosphite, 2.0 g, 13.20 mmol benzyl carbamate, 2.38 mL, 19.80 mmol phenylacetaldehyde and 2.0 mL glacial acetic acid for 4 h at 100 °C in an oil bath. The diphenyl phosphonate formed was hydrolyzed with 0.40 N NaOH, acidified with conc. HCl, filtered, and purified by column chromatography using 9:1 chloroform–methanol mixture. FTIR:- 1301 cm^{-1} (P═O stretching), 946 cm^{-1} (P—OH stretching) and 1252 cm^{-1} (P—O—benzyl stretching).

The transition state analog phenyl-1-benzyloxycarbonylamino-4-methoxybenzyl phospohonate was also prepared by the same method using 4-methoxybenzaldehyde instead of phenylacetaldehyde for a comparison [15].

2.3. Synthesis of TSA imprinted enzyme mimics and non-imprinted control polymers

The enzyme mimic polymer **C1** was prepared by radical initiated bulk polymerization of 223 mg, 10 mmol, of monomer *N*-methacryloyl-L-histidine (MALH) and 3.4 mL, 90 mmol, of the crosslinking agent EGDMA in presence of 205.5 mg, 0.50 mmol TSA-A in 40 mL DMSO for 6 h at 80 °C. The template was completely leached out by washing with methanol and then subjected to Soxhlet extraction with chloroform. The polymer obtained was collected and dried over vacuum.

Enzyme mimics **C2–C7** were also synthesized as per the same procedure. The corresponding non-imprinted control polymers **CPs** were also prepared by the same procedure in the absence of TSA. The total amino content in the polymer mimics were estimated by ninhydrin reagent. The morphology of the polymers was characterized SEM analysis.

2.4. Synthesis of the substrate Z-L-*phenylalanine*-p-*nitroanilide* (Z-L-*Phe-PNA)*

The substrate *Z*-L-Phe-PNA was synthesized by dissolving 2.99 mg (0.01 mol) *Z*-L-phenylalanine and 1.38 mg (0.01 mol) *p*-nitroaniline in 30 mL ethyl acetate and the solution was stirred on a magnetic stirrer in an ice-water bath for half an hour. A solution of 2.06 mg (0.01 mol) DCC in 30 mL ethyl acetate was added drop wise and the reaction mixture was stirred for 30 min in the ice water bath and the stirring was continued for further 3 h at room temperature. The DCU formed was filtered off and the filtrate was evaporated in vacuum. The residue obtained was recrystallized from hot ethanol containing 1% acetic acid. The substrates, t-Boc/Nphth/Fmoc-L-phenylalanyl-*p*-nitroanilide and *Z*-L-alanyl-*p*-nitroanilide were also prepared following the same procedure.

2.5. Amidolysis of Z-L-*phenylalanine*-p-*nitroanilide* (Z-L-*Phe-PNA) using TSA imprinted and non-imprinted enzyme mimics: general procedure*

A suspension of 10 mg chymotrypsin mimic **C1** (0.00647 mmol) was suspended in 5 mL acetonitrile–Tris HCl buffer (1:9 by volume, pH 7.75) in a reagent bottle and 271 mg, 0.647 mmol of the substrate *Z*-Phe-PNA in 50 mL acetonitrile was added. The reaction mixture was placed in a water bath shaker at 45 °C and shaken gently. Amidolysis of *Z*-Phe-PNA was followed by monitoring the absorbance of released *p*-nitroaniline spectrophotometrically at 374 nm in the framework of Michaelis–Menten kinetics and the reaction was monitored for two days. A blank reaction was also carried out in the absence of the enzyme mimic. From the absorbance data, the rate constants and percentage amidolysis were evaluated. Amidase activity of the mimics **C2–C7** was evaluated in a similar manner.

2.6. Regeneration and reusability of the spent polymer

The spent enzyme mimics were collected by filtration, washed simultaneously with distilled water and Tris–HCl buffer (pH 7.75) and dried under vacuum. In the second cycle the amidolytic reaction was carried out in fresh Tris–HCl buffer solution. Catalytic amidolysis was repeated for 6 cycles.

3. Results and discussion

3.1. Synthesis of TSA- A: *phenyl-1-(*N-*benzyloxycarbonylamino)-2-(phenyl)ethyl phosphonate*

The TSA, which has more structural resemblance with the substrate, was synthesized using triphenyl phosphite, benzyl carbamate and phenylacetaldehyde. The TSA synthesized possesses Z group of the substrate and the "specificity determinant" – $C_6H_5CH_2$ group – of chymotrypsin.

The TSA synthesized was characterized by FTIR and NMR spectroscopic techniques. FTIR of the TSA exhibited bands at 1301, 946 and 1252 cm^{-1} corresponding to P═O stretching, P—OH stretching and P—O—benzyl stretching respectively. The ^{1}H NMR spectra showed singlets at δ 1.73 and 5.21 corresponding to OH group and CH_2 of Z group respectively. The methylene protons (CH—CH_2) appeared at δ 2.81 as doublet and the alkyl CH resonated at δ 4.09 as multiplet. The NH proton appeared as doublet at 6.01 ppm. The 15 aromatic protons showed a multiplet at 6.5–7.5 ppm.

3.2. Synthesis of TSA imprinted and non-imprinted polymers

The molecularly imprinted polymers were prepared by radical initiated bulk polymerization method using the functional monomers, template TSA and the cross linker EGDMA. The monofunctional mimics **(C1–C3)** were synthesized using *N*-methacryloyl-L-histidine (MALH)/*N*-methacryloyl-L-aspartic acid (MALA)/*N*-methacryloyl-L-serine (MALS) respectively with EGDMA and TSA-A in the molar ratio 1:9:0.5.

Similarly the bifunctional enzyme mimics **(C4–C6)** were prepared using functional monomers *N*-methacryloyl-L-histidine, *N*-methacryloyl-L-aspartic acid and *N*-methacryloyl-L-serine**—C4** with MALH and MALA, **C5** with MALH and MALS and **C6** with MALA and MALS. The monomers, EGDMA and TSA-A were in the molar ratio 0.5:0.5:90:0.5 (Table 1). Trifunctional mimic **C7** was obtained

Table 1
Details of the synthesis of enzyme mimics **C1–C7**.

Polymer catalysts	TSA (mg)	MALH (mg)	MALA (mg)	MALS (mg)	EGDMA (mL)	Total amino acid content (mmol/g)
C1	205.5	223	–	–	1.70	0.647
C2	205.5	–	201	–	1.70	0.650
C3	205.5	–	–	173	1.70	0.651
C4	205.5	111.5	100.50	–	1.70	0.564
C5	205.5	111.5	–	86.5	1.70	0.582
C6	205.5	–	100.50	86.5	1.70	0.578
C7	205.5	74.33	67	57.67	1.70	0.542

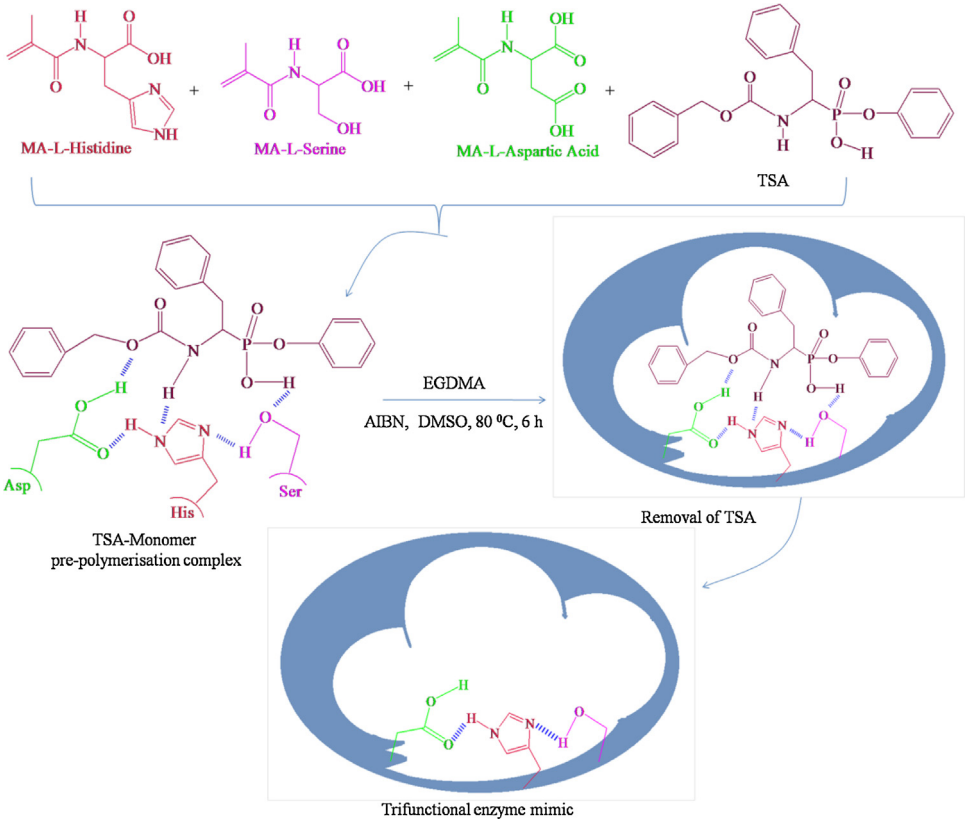

Scheme 1. Scheme for the synthesis of trifunctional enzyme mimic.

from the three monomers, the crosslinker and TSA-A in the molar ratio 0.33:0.33:0.33:9:0.5 (Scheme 1).

The non-imprinted control polymers **(CPs)** were also synthesised in the same molar ratios of monomers and the cross linker without the TSA molecule. The total functional groups in the mimics-imidazole, carboxyl and hydroxyl-were estimated by cleaving the amino acids from the methacrylic backbone by refluxing with HCl followed by treating with ninhydrin reagent [16].

The morphology of the imprinted and non-imprinted polymers was assessed by SEM analysis. The SEM photograph of the imprinted enzyme mimic **C7** shows many cavities formed after the removal of the TSA molecules. Nevertheless, the corresponding non-imprinted control polymer **CP** exhibited relatively smooth surface without cavities (Fig. 1).

3.3. *Catalytic amidolysis of Z-L-Phe-PNA, evaluation of kinetic parameters*

The hydrolysis of amide linkage is slow compared to the hydrolysis of ester linkage. There are so many reports on molecularly imprinted polymer catalyzed esterolysis [17–22]. but, amidolysis using transition state analog imprinted enzyme mimics is less reported. Amidolysis of *Z*-L-Phe-PNA was taken as the model reaction for evaluating the catalytic properties of the enzyme mimics. Ester hydrolytic reactions using enzyme mimics were reported to be pseudo first order. Investigations revealed that the amidase activity of the enzyme mimics is also found to follow pseudo first order kinetics and the rate constants were evaluated using the equation, $k = \ln[A_\infty/(A_\infty - A_t)]$, where A_∞ is the absorbance at infinite time and A_t is the absorbance at time t (Fig. 2). The rate acceleration of the polymer catalyst compared to the blank hydrolysis was evaluated in terms of the ratio $k_{obs.}/k_{uncat.}$ and the catalytic efficiency of the polymer catalysts was measured as $k_{cat.}$ which is calculated using the equation

$$k_{cat.} = \frac{k_{obs.} - k_{uncat.}}{\text{functional groups}}.$$

The imprinting efficiency of the polymer catalysts is expressed in terms of k_{MIP}/k_{CP}. The rates of amidolysis observed in the presence of imprinted and non-imprinted polymers are compared with the rate of uncatalyzed hydrolysis (blank) to evaluate the catalytic competence of the mimics. The rate constant for the uncatalyzed reaction is found to be $0.52 \times 10^{-4}\,\text{min}^{-1}$. Compared to the blank, the imprinted mimic **C1** and the correspond-

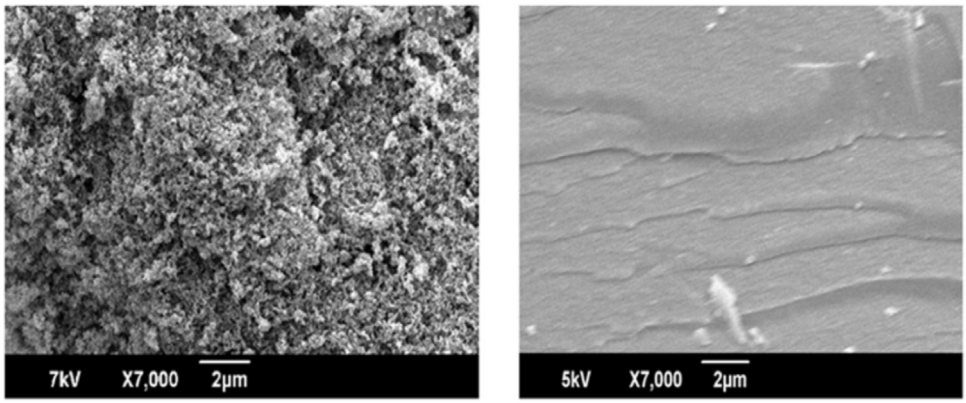

Fig. 1. SEM picture of the imprinted and control polymer.

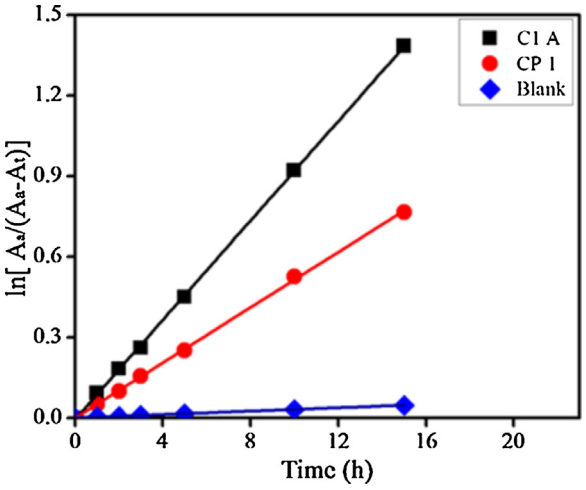

Fig. 2. Kinetics of amidolysis of *Z*-L-Phe-PNA with enzyme mimic **C1,** control polymer **CP1** and the uncatalyzed reaction.

ing non-imprinted control polymer show higher catalytic rate constants—1.54×10^{-3} min^{-1} and 0.65×10^{-3} min^{-1} respectively.

In the imprinted polymer, the imprint of the "phospohonate TSA" provides a site complementary to the tetrahedral transition state of amidolysis. The effective hydrogen bonding between the transition state and the imidazole units makes the imprinted polymer catalytically more efficient than the non-imprinted polymer in which the functional monomers are randomly distributed due to the lack of the TSA.

3.4. Effect of the structure of TSA on catalytic amidolysis

The selectivity and efficiency of the imprinted enzyme mimics depend on the structural complementarity between the catalytic cavity and the T.S of amidolysis. Removal of the template molecule provides a cavity, which matches the physicochemical properties of the template species. If the imprinted TSA has a closer structural resemblance to the substrate, the corresponding enzyme mimic will exhibit high catalytic activity.

The effect of the structure of the imprinted TSA on the catalytic activity of the enzyme mimic was investigated by following the amidolytic reaction of *Z*-Phe-PNA in presence of enzyme mimic **C1** with different transition state analogs—TSA-A, TSA-B and TSA-C (phenethyl boronic acid) (Fig. 3).

2-Phenethaneboronic acid is reported to be a potential inhibitor of chymotrypsin in the hydrolysis of methyl hippurate and acts as transition state analog for chymotrypsin catalyzed hydrolytic reactions [23]. Hence we have prepared polymer catalysts **C1** with phenethyl boronic acid as the template.

The enzyme mimic **C1,** with the imprints of TSA-A shows maximum activity with a $k_{cat.}$ value of 15.77×10^{-2} min^{-1} $mmol^{-1}$ and 35% amidolysis. The mimic having imprints of TSA-B showed a $k_{cat.}$ value of 5.63×10^{-2} min^{-1} $mmol^{-1}$ and 20% amidolysis. The $k_{cat.}$ value and percentage amidolysis of TSA-C imprinted polymer are 2.13×10^{-2} min^{-1} $mmol^{-1}$ and 19% respectively. TSA-A has more structural resemblance with the substrate *Z*-Phe-PNA having the specificity determining $C_6H_5CH_2$ group and TSA-C resembles the substrate least. The rate acceleration $k_{obs.}/k_{uncat.}$ shown by TSA-A, B and C imprinted **C1** enzyme mimics are 29.62, 16.96 and 10.77 respectively. The results are given in Table 2. The saturation time for the three **C1** polymers was 50, 120 and 150 h respectively. Hence, TSA-A was selected for the preparation of enzyme mimics for further investigations.

3.5. Co-operative effect of functional monomers on amidolysis

The individual and combined effects of imidazole, carboxyl and hydroxyl groups in the chymotrypsin mimics on the amidolysis of *Z*-L-Phe-PNA were analyzed. Amidolysis of Z-L-Phe-PNA by the mimic C7 is given in Scheme 2. Among the monofunctional enzyme mimics, the rate acceleration $k_{obs.}/k_{uncat.}$ values for **C1**, **C2** and **C3** mimics are 29.62, 12.50 and 15.00 respectively. The enzyme efficiency $k_{cat.}$ value for **C1** mimic with imidazole units is found to be 7.88 times that of **C2** polymer with aspartic acid residues and 3.94 times the value of **C3** polymer with serine residues.

The $k_{obs.}/k_{uncat.}$ values for the bifunctional mimics **C4, C5** and **C6** were evaluated to be 41.53, 45.77 and 15.96 respectively. The enzyme efficiency $k_{cat.}$ (0^2 min^{-1} $mmol^{-1}$) value for **C5** mimic with histidine and serine units is found to be 1.10 times that of **C4** polymer with histidine and aspartic acid residues and 5.96 times the value for **C6** polymer with serine and aspartic acid monomers. The $k_{cat.}$ value of mimic **C4** is 1.84 and 14.54 times the value of **C1** and **C2** respectively. Similarly, the catalytic efficiency of **C5** is 2.03 and 7.99 times that of **C1** and **C3**. The polymer catalyst **C6** is 2.68 and 1.34 times efficient than **C2** and **C3**. The increase in the catalytic efficiency of the bifunctional mimics compared to the corresponding monofunctional mimics can be explained as due to the cooperative effects of functional groups. The **C5** copolymer is the best bifunctional enzyme mimic, in which the basic nitrogen of imidazole moiety takes the acidic proton from the hydroxyl group of serine to

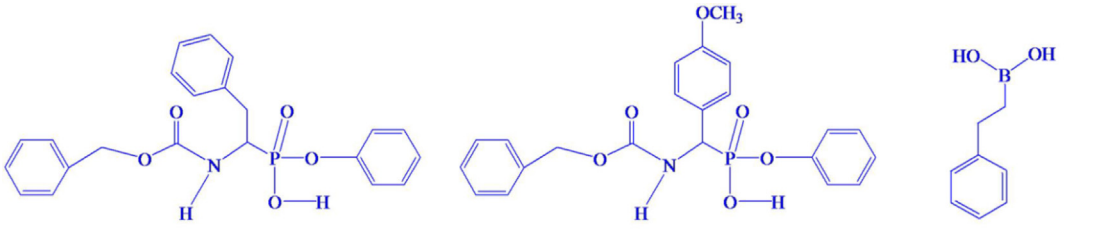

Fig. 3. Structure of transition state analogs A, B & C.

Table 2
Kinetic parameters for the amidolysis of *Z*-L-Phe-PNA with TSAs A, B & C.

Enzyme mimics	TSA	10^3 $k_{obs.}$ (min^{-1})	$k_{obs.}/k_{uncat.}$	10^2 $k_{cat.}$ (min^{-1} $mmol^{-1}$)	Saturation time (h)
C1	A	1.54	29.62	15.77	50
	B	0.83	15.96	5.36	120
	C	0.56	10.77	2.13	150

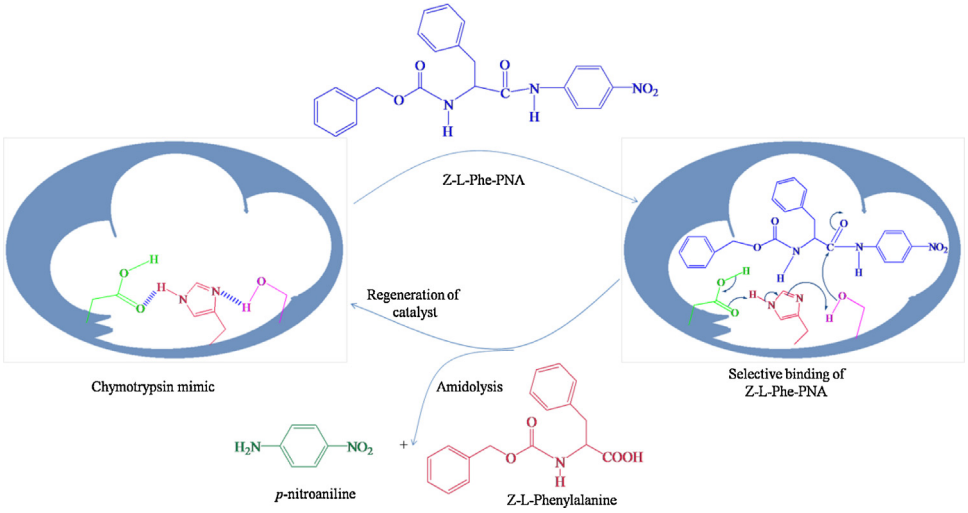

Scheme 2. Amidolysis of *Z*-L-Phe-PNA using enzyme mimic **C7**.

enhance its nucleophilicity. In the bifunctional polymer **C4** interactions were provided by the incorporation of the carboxylic group of aspartic acid, which was expected to co-ordinate to the acidic proton on imidazole nitrogen, provides a 'proton shuttle' to assist amidolysis. However, the polymer catalyst **C6** not having histidine residues is less efficient than the mimic **C1** with histidine units. These results clearly show that the key catalytic site in the polymer mimics is the imidazole moiety of histidine.

The $k_{cat.}$ value of trifunctional mimic **C7** is observed to be 3.98 times that of monofunctional mimic **C1** and about 2 times that of bifunctional mimics **C4** and **C5**. Enzyme mimics **C2**, **C3** and **C6** are found to be much less efficient than **C7**.

The ratio k_{MIP}/k_{CP} is defined as the imprinting efficiency. The k_{MIP}/k_{CP} values of the mimics **C1–C7** were evaluated and the results are given in Table 3. The higher values of imprinting efficiency for **C4** (2.60), **C5** (2.74) and **C7** (4.22) can be explained as due to the cooperative effect of the functional groups in the catalytic sites.

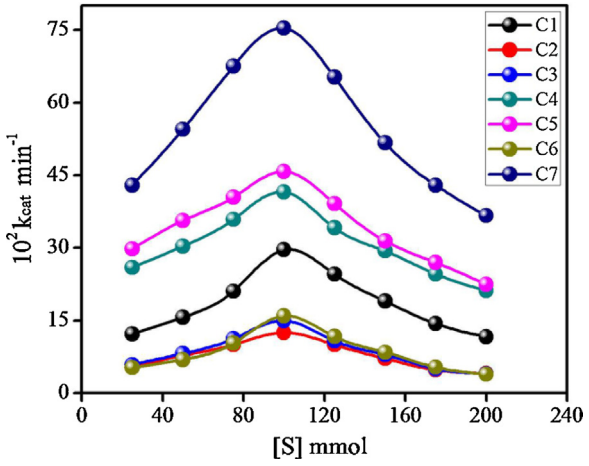

Fig. 4. Effect of substrate concentration on the amidolysis of *Z*-L-Phe-PNA.

3.6. Michaelis–Menten kinetics

The Michaelis–Menten kinetics of the enzyme mimics was investigated by following the kinetics of the amidolysis of *Z*-L-Phe-PNA. The reaction was carried out with different substrate concentrations (Fig. 4). The optimum molar ratio was found to

Table 3
Kinetic parameters for the amidolysis of *Z*-L-Phe-PNA by TSA imprinted enzyme mimics supporting co-operative effect of functional monomers.

Enzyme mimic	10^3 $k_{obs.}$ (min^{-1})	$k_{obs.}/k_{uncat.}$	k_{MIP}/k_{CP}	10^2 $k_{cat.}$(min^{-1} mol^{-1})	Saturation time (h)
C1	1.54	29.62	2.37	15.77	50
C2	0.65	12.50	1.12	2.00	120
C3	0.78	15.00	1.08	4.00	120
C4	2.16	41.53	2.60	29.08	40
C5	2.38	45.77	2.74	31.96	35
C6	0.83	15.96	1.15	5.36	120
C7	3.92	75.38	4.22	62.70	22

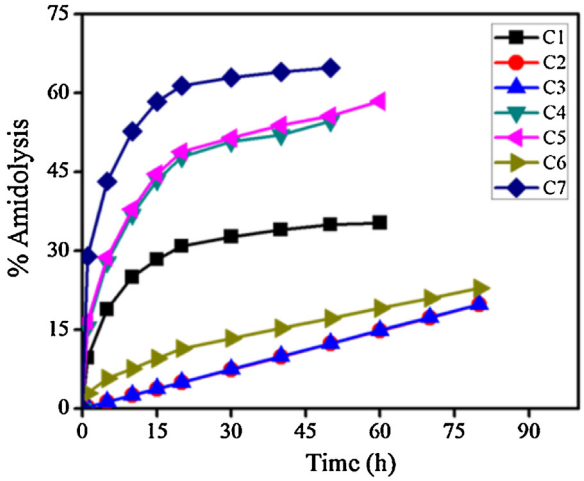

Fig. 5. Percentage amidolysis vs. time using enzyme mimics **C1–C7**.

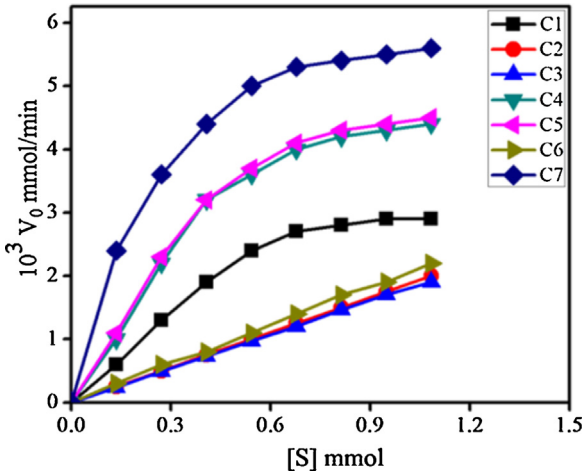

Fig. 6. Michaelis–Menten plots for the hydrolysis of *Z*-L-Phe-PNA with enzyme mimics **C1–C7.**

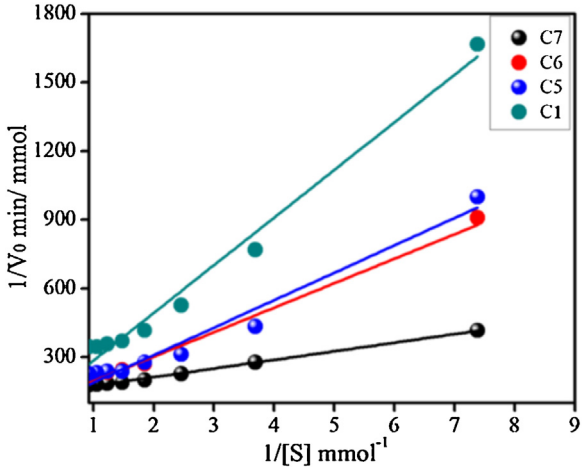

Fig. 7. Lineweaver–Burk plots for amidolysis of *Z*-L-Phe-PNA using chymotrypsin mimics.

be 1:100 and beyond this concentration catalytic activity was decreased due to substrate inhibition.

Fig. 5 is a plot of percentage amidolysis vs. time for the reaction at enzyme mimic/substrate molar ratio 1:100.

The reaction obeying Michaelis–Menten kinetics exhibits initial burst kinetics and reaches saturation [16]. The amidolysis with mimics **C1, C4, C5** and **C7** follows Michaelis–Menten kinetics under excess substrate condition (1:100). The monofunctional mimics **C1**and **C3** and bifunctional mimic **C6** behave only as nucleophilic catalysts in the amidolysis. Here also it is observed that only the mimics with histidine moieties obey Michaelis–Menten kinetics.

Fig. 6 shows Michaelis–Menten plots of initial velocity (V_0) vs. substrate concentration [*S*] for the enzyme mimics **C1–C7** with different catalyst to substrate ratios in the range 1:25–1:200.

The hyperbolic curves obtained for the initial velocity (V_0) vs. substrate concentration [*S*] data shows good adherence to the Michaelis–Menten saturation model for the mimics **C1**, **C4**, **C5** and **C7** with histidine moieties. The polymer catalysts obeying Michaelis–Menten kinetics are described as chymotrypsin mimics and the kinetic parameters 1/Km and V_{max}/Km are cited to characterize their amidase activity. The double reciprocal plots of $1/V_0$ vs. $1/S$ for **C1, C4, C5** and **C7** are shown in Fig. 7.

Values of V_{max} (reciprocal of *Y*-intercept) were evaluated from plots. The inverse of the Michaelis constant 1/Km is an indicator of the affinity of the enzyme for its substrate i.e., a low Km (or high 1/Km) corresponds to high affinity for binding the substrate. In the present case, 1/Km represents the affinity of the enzyme mimics for the substrate *Z*-L-Phe-PNA. The results are given in Table 4. The substrate affinity of the polymer **C7** toward *Z*-L-Phe-PNA is 9.89 times the affinity of monofunctional **C1** and 4.4 and 6.31 times the affinity of bifunctional **C4** and **C5** mimics.

The mimic **C7** exhibits higher enzyme catalytic efficiency (V_{max}/Km) for *Z*-Phe-PNA. It is clear from the results that the TSA imprints favor the co-operative action amongst hydroxyl, carboxyl and imidazole groups on the polymer support, similar to chymotrypsin.

3.7. *Enantioselectivity of enzyme mimics on amidolysis*

The enantioselectivity of the imprinted mimics and non-imprinted control polymers was studied in the amidolysis of *Z*-L/D-Phe-PNA. The ratio $k^{L}_{cat.}/k^{D}_{cat.}$ is a measure of the enantioselectivity of the enzyme mimics and the values are calculated for different polymer catalysts obeying Michaelis–Menten kinetics. The enantioselectivity of the TSA imprinted enzyme mimic arises due to the interaction of L-monomers with L-TSA in the pre-polymerization complex [4,5,24,25]. Hence the enzyme mim-

Table 4
Kinetic data obtained from Lineweaver–Burk plots.

Enzyme mimic	$1/V_{max}$ (min mmol^{-1})	Km/V_{max} (min)	10^2 V_{max} (mmol min^{-1})	Km (mmol)	1/Km (mmol^{-1})	10^3 V_{max}/Km (min^{-1})
C1	77.77	208.05	1.29	2.68	0.37	4.81
C4	69.77	119.78	1.43	1.71	0.58	8.36
C5	88.31	106.97	1.13	1.21	0.83	9.34
C7	137.68	37.61	0.73	0.27	3.66	26.74

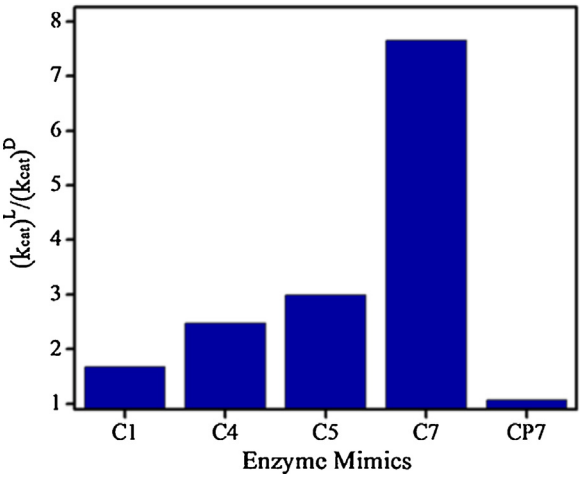

Fig. 8. Enantioselectivity of the enzyme mimics in the amidolysis of Z-L & Z-D-Phe-PNA.

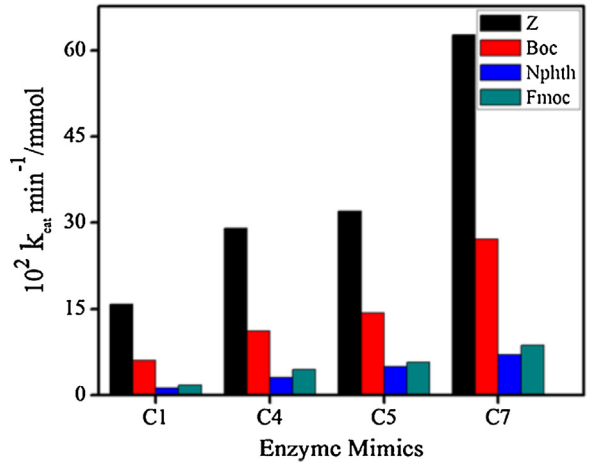

Fig. 9. Amidolysis of Phe-PNA having different Nα-protecting groups.

ics show selectivity toward Z-L-Phe-PNA over the D-enantiomer. The results are shown in Fig. 8.

From Fig. 8, it is clear that the enantioselectivity of enzyme mimics varies from 1.68(**C1**) 7.65(**C7**). The catalyst **C7** exhibits highest enantioselectivity due to the formation of "shape and stereo-selective" recognition sites in the macroporous polymer matrix during molecular imprinting. The trifunctional mimic **C7** permits an "exact fit" of Z-L-Phe-PNA in the three dimensional recognition sites formed from the most stable "TSA-monomer pre-polymerization complex" through effective H-bonding interactions between L-TSA and the L-monomers during imprinting. Moreover, the super crosslinked nature of 90% EGDMA-crosslinked mimic keeps the catalytic cavity intact facilitating the selective binding of the L-enantiomer. The control polymers **CP** do not exhibit considerable enantioselectivity due to lack of recognition sites in the polymer matrix. The hydrolysis of the D-enantiomer even with the most efficient mimic **C7** does not obey Michaelis–Menten kinetics and the plot obtained is found to be linear.

3.8. Effect of substrate selectivity of enzyme mimics

To investigate the role of size and shape of the imprinted cavity in governing the kinetics of amidolysis, the reaction was carried out with L-Phe-PNA with different amino protecting groups using both imprinted enzyme mimics and control polymers. The hydrolysis of Z-, Boc-, Nphth- and Fmoc-L-Phe-PNA with the mimics **C1**, **C4**, **C5** and **C7** were carried out and the results are shown in Fig. 9. The substrate selectivity of the imprinted polymers were determined in terms of $k_{cat.}$ and the selectivity is observed in the order Z-L-Phe-PNA > t-Boc-L-Phe-PNA > Fmoc-L-Phe-PNA > Nphth-L-Phe-PNA. The extremely precise recognition sites created in the polymer matrix, during the removal of the TSA is accountable for the high substrate recognition supremacy. The imprinted polymer catalyst kept the structure of the TSA in the memory and could recognize structurally similar substrate, Z-L-Phe-PNA [24]. The deviation from the structure of TSA decreases the binding efficiency of the substrate in the active site of the enzyme mimic. The $k_{cat.}$ values calculated for the mimic **C7** are found to be 75.38 (Z-L-Phe-PNA), 27.12 (t-Boc-L-Phe-PNA), 7.01 (Nphth-L-Phe-PNA) and 8.67 (Fmoc-L-Phe-PNA). The other mimics also exhibited the same trend (Fig. 9). The results are supported by the $k_{cat.}$ values for non-imprinted control polymers, which did not exhibit any substrate selectivity. The $k_{cat.}$ (10^2 min^{-1} mmol^{-1}) values observed for the best control polymer **CP7** are 14.91 (Z-L-Phe-PNA), 14.28 (t-Boc-L-Phe-PNA), 13.82 (Nphth-L-Phe-PNA) and 13.28 (Fmoc-L-Phe-PNA).

3.9. Specificity of enzyme mimics

Chymotrypsin exhibits specificity for esters and amides comprising of aromatic hydrophobic amino acids like phenylalanine or tyrosine residues as a part of the carbonyl group. The aromatic side chain is accommodated in the hydrophobic pocket of the active site during hydrolysis [23,26]. To study the specificity of the enzyme mimics, amidolytic reactions of two different amino acid anilides Z-L-Phe-PNA and Z-L-Ala-PNA were carried out. The specificity values of the mimics were calculated as the ratio $k_{cat}^{phe}/k_{cat}^{Ala}$. The maximum value for specificity is observed for the trifunctional mimic **C7** (5.31). Other mimics also exhibited specificity toward Z-L-Phe-PNA (Fig. 10).

The control polymers did not show any significant substrate specificity. The specificity of the enzyme mimics can be explained as due to the presence of hydrophobic pocket created by the "$C_6H_5CH_2$ group" of the TSA in the polymer matrix.

3.10. Comparison with natural chymotrypsin

The kinetics of amidolysis of Z-L-Phe-PNA catalyzed by trifunctional mimic **C7** was compared with the amidolysis catalyzed by natural chymotrypsin (Fig. 11). The mimic **C7** shows 62% completion of the reaction with a saturation time of 22 h. With natural chymotrypsin, the reaction reached 80% completion in 45 min. The Km value of chymotrypsin catalyzed amidolysis at room temperature was evaluated from the double reciprocal plot by taking various substrate concentrations in the range of 5–30 μm. The Km value is found to be 0.1 μm which is 2.7×10^3 times the value of

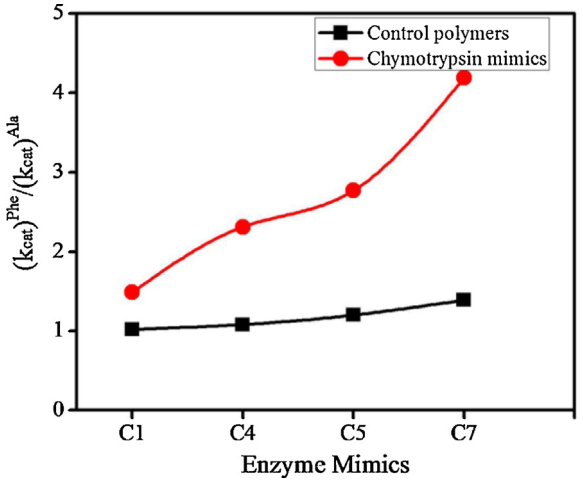

Fig. 10. Substrate specificity of the enzyme mimics in the amidolytic reactions of *Z*-L-Phe-PNA and *Z*-L-Ala- PNA.

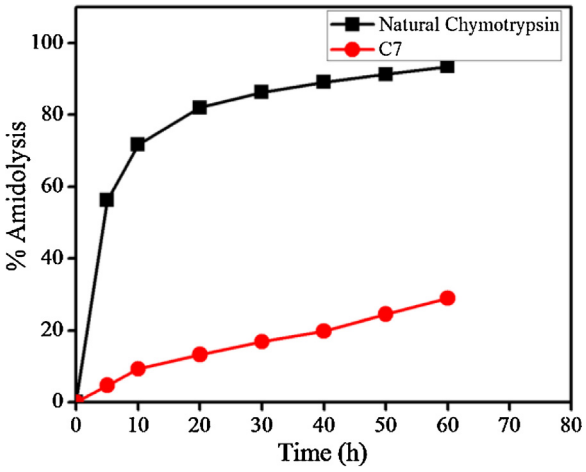

Fig. 11. Comparison between natural chymotrypsin and **C7** mimic.

the mimic **C7** at 45 °C. Michaelis–Menten behavior of **C7** is not significant in the initial period compared to the natural enzyme due to the heterogenic nature of the reaction and the time required for the solvation of the polymer catalyst.

3.11. Thermal stability

The thermal stability of the enzyme mimic was investigated by incubating the imprinted mimics for 4 h at a range of temperatures 90–150 °C. By measuring the catalytic parameters, it is found that, the enzyme mimics are stable up to 130 °C and then the catalytic activity gets decreased (Fig. 12). Natural chymotrypsin is denatured in the temperature range of 45–55 °C.

The enzyme mimics exhibit almost same catalytic activity even after one-year shelf life. Moreover, the mimics are much more cost-effective and hence the enzyme mimics are economic.

3.12. Regeneration and reusability of the enzyme mimics

We have investigated the reusability of the spent imprinted enzyme mimics by carrying out amidolytic reaction several cycles after regenerating the polymer. It was observed that the enzyme mimics regenerated could be used for five cycles of amidolysis without much loss in catalytic activity. The results are given in Table 5. The reusability of the enzyme mimics in the amidolysis of *Z*-L-Phe-PNA was assessed at pH 7.75 with enzyme mimic-substrate molar ratio 1:100. The rate acceleration $k_{obs.}/k_{uncat.}$ of the reaction was evaluated for each cycle.

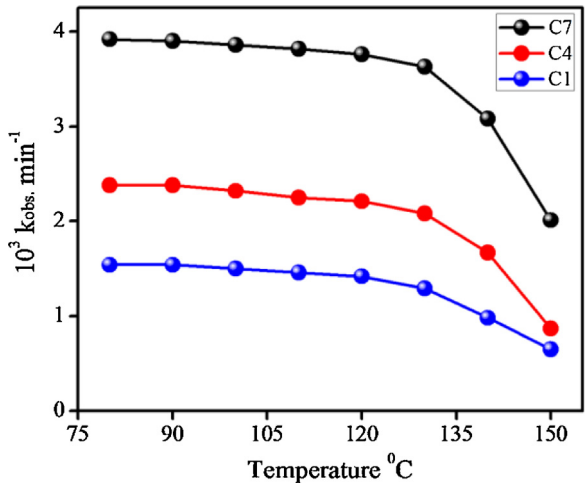

Fig. 12. Thermal stability of chymotrypsin mimics.

Table 5
Reusability of the spent enzyme mimic (**C7**).

No. of cycles	$k_{MIP}/k_{uncat.}$	Saturation time (h)	% activity
1	7.54	22	100
2	7.51	22	99
3	7.46	23	98
4	7.38	23	97
5	7.23	25	95
6	7.36	27	92

The activity of the fresh enzyme mimic was considered as the control with 100% activity. After the fifth cycle, a reduction in catalytic activity of 5% was observed which can be explained as mainly due to the deformation of some of the substrate recognition sites. Reusability makes the enzyme mimic more economic.

4. Conclusion

Phenyl-1-(*N*-benzyloxycarbonylamino)-2-(phenyl)ethyl phosphonate imprinted polymer catalysts were found to possess enzyme-like catalytic properties and obeyed Michaelis–Menten kinetics. The catalysts exhibited good enantioselectivity, memory effect and substrate specificity in the amidolysis of phenylalanine-*p*-nitroanilides. High thermal stability, increased shelf-life and reusability make the enzyme mimics highly economic compared to the natural chymotrypsin. Investigations on the hydrolysis of peptides with phenylalanine and tyrosine residues using the enzyme mimics are going on in our laboratory.

Acknowledgements

The authors gratefully acknowledge the support from CSIR for awarding junior and senior research fellowships to Divya Mathew. We are also thankful to IIRBS-Mahatma Gandhi University for providing facilities for spectral analysis and School of Biosciences for providing facilities for incubation studies.

References

[1] A. Leonhardt, K. Mosbach, React. Funct. Polym. 6 (1987) 285–290.
[2] K. Ohkubo, Y. Urata, S. Hirota, J. Mol. Catal. A: Chem. 87 (1994) L21–L24.
[3] K. Ohkubo, Y. Urata, S. Hirota, J. Mol. Catal. A: Chem. 93 (1994) 189–193.
[4] B. Sellergren, K.J. Shea, Tetrahedron: Asymmetry 5 (1994) 1403–1406.

[5] B. Sellergren, R.N. Karmalkar, K.J. Shea, J. Org. Chem. 65 (2000) 4009–4027.
[6] Y. Kawanami, T. Yunoki, A. Nakamura, J. Mol. Catal. A: Chem. 145 (1999) 107–110.
[7] E. Toorisaka, M. Yoshida, K. Uezu, Chem. Lett. 5 (1999) 387–388.
[8] S.A. Zaidi, Electrophoresis 34 (2013) 1375–1382.
[9] J.M. Kim, K.D. Ahn, G. Wulff, Macromol. Chem. Phy. 202 (2001) 1105–1108.
[10] M. Subat, A.S. Borovik, B.J. König, J. Am. Chem. Soc. 126 (2004) 3185–3190.
[11] R.L. Schowen, in: J.F. Liebman, A. Greenberg (Eds.), Mechanistic Principles of Enzyme Activity, VCH, New York, 1988.
[12] M.L. Bender, F.J. Ke'zdy, J. Am. Chem. Soc. 86 (1964) 3704–3714.
[13] T. Kunitake, Y. Okahata, Adv. Polym. Sci. 20 (1976) 159–805.
[14] M.L. Bender, G.R. Schonbaum, G.A. Hamilton, J. Polym. Sci. 49 (1961) 75–103.
[15] K. Ohkubo, Y. Urata, S. Hirota, Y. Funakoshi, T. Sagawa, S. Usui, K. Yoshinaga, J. Mol. Catal. A: Chem. 101 (1995) L111–L114.
[16] B.S. Lele, M.G. Kulkarni, R.A. Mashelkar, React. Funct. Polym. 40 (1999) 215–229.
[17] G. Wulff, T. Gross, R. Schonfeld, Angew. Chem. Int. Ed. Engl. 36 (1997) 1962–1964.
[18] K.D. Robinson, K. Mosbach, J. Chem. Soc. Chem. Commun. 28 (1989) 969–970.
[19] K. Ohkubo, Y. Urata, K. Yoshinaga, Polymer 35 (1994) 5372–5376.
[20] E. Toorisaka, K. Uezu, M. Goto, S. Furusaki, Biochem. Eng. J. 14 (2003) 85–89.
[21] K. Ohkubo, K. Sawakuma, T. Sagawa, Polymer 42 (2001) 2263–2266.
[22] R.N. Karmalkar, M.G. Kulkarni, R.A. Mashelkar, Macromolecules 29 (1996) 1366–1368.
[23] K.A. Koehler, G.E. Lienhard, Biochemistry 10 (1971) 2477–2483.
[24] K. Ohkubo, K. Sawakuma, T. Sagawa, J. Mol. Catal. A: Chem. 165 (2001) 1–7.
[25] K. Ohkubo, Y. Funakoshi, T. Sagawa, Polymer 37 (1996) 3993–3995.
[26] T.A. Steitz, R. Henderson, D.M. Blow, J. Mol. Biol. 46 (1969) 337–348.